

Niu, Y. & R. Hékinian

Ridge suction drives plume-ridge interactions (Chapter 9), *In Oceanic Hotspots*, edited by R. Hékinian & P. Stoffers, Springer-Verlag, New York, p. 285-307, 2004.

# Ridge Suction Drives Plume-Ridge Interactions

Y. Niu · R. Hekinian

## 9.1 Introduction

Geological processes are consequences of the Earth's thermal evolution. Plate tectonics, which explain geological phenomena along plate boundaries, elegantly illustrate this concept. For example, the origin of oceanic plates at ocean ridges, the movement and growth of these plates, and their ultimate consumption back into the Earth's interior through subduction zones provide an efficient mechanism to cool the Earth's mantle, leading to large-scale mantle convection. Mantle plumes, which explain another set of global geological phenomena, cool the Earth's deep interior (probably the Earth's core) and represent another mode of Earth's thermal convection (e.g., Davies and Richards 1992). Plate tectonics and plume tectonics are thus genetically independent from each other. However, when the rising plumes approach the lithospheric plates, interactions between the two inevitably result. Such interactions are most prominent near ocean ridges, where the lithosphere is thin and the effect of mantle plumes is best revealed. "Plume-ridge interaction" has been a hot topic in recent years, and much effort has been expended in this area aimed at understanding the geological, geochemical, and geodynamic consequences (Schilling et al. 1983, 1994, 1995, 1996, 1999; Schilling 1991; Feighner and Richards 1995; Ito and Lin 1995a,b; Ito et al. 1996; Kincaid et al. 1995, 1996; Ribe 1996; Sleep 1996; Haase and Devey 1996; Hekinian et al. 1996, 1997, 1999; Pan and Batiza 1998; Niu et al. 1999; Graham et al. 1999; Maia et al. 2000; Georgen et al. 2001; Haase 2002).

In this study, instead of reviewing details of existing models, we present our new perspectives on the geochemical and geological consequences of plume-ridge interactions in the form of schematic models. These models differ from most common perceptions, but are consistent with observations and comply with simple physics. We focus on first-order observations and stress the importance of several fundamental concepts and variables required to fully understand the "expression" and "intensity" of plume-ridge interactions. These include: (1) what mantle plumes are; (2) the nature and composition of plume sources; (3) the actual role of ocean ridges; (4) the effect of plate separation rate; and (5) plume-ridge distance. We illustrate these concepts/variables with representative examples.

## 9.2 Concepts

### 9.2.1

#### Mantle Plumes:

#### Deep-Rooted Hot Materials or Wet Shallow Mantle Melting Anomalies?

The theory of plate tectonics, by its definition, explains tectonic activities along plate boundaries between two adjacent plates. For example, volcanism at ocean ridges and overlying subduction zones is the consequence of plate tectonics. However, volcanism occurring away from plate boundaries cannot be explained by plate tectonics theory. This “intraplate” volcanism is often interpreted as resulting from hotspots or mantle plumes. Volumetrically large and temporally long-lived intraplate volcanism represented by the islands of Hawaii in the Pacific, the Azores in the Atlantic and the Kerguelen plateau in the southern ocean may indeed be hotspots genetically associated with deep-rooted mantle plumes (Morgan 1971, 1981; Duncan and Richards 1991). However, other intraplate volcanism such as Cenozoic volcanic activities widespread in eastern Australia (e.g., Johnson ed. 1989) and eastern China (Deng et al. 1998; Zhang et al. 1998), the well-known Cameroon volcanic line (Halliday et al. 1988) and numerous seamounts scattered throughout much of the Earth’s ocean floor (Batiza 1982) away from any plate boundaries are likely to be melting anomalies resulting from easily melted fertile mantle source materials (enriched in volatiles, alkalis and other incompatible elements) in the shallow asthenosphere. The latter may be more appropriately termed “wet spots” (e.g., Green and Falloon 1998). We must emphasize, however, that we do not yet at present have sufficient data to draw a clear distinction between “hot-spots” and “wet spots”. It is possible that some or many of the so-called hotspots may prove to be wet spots when more relevant data become available. In the following discussion, we simply use the terms “hotspots” or “mantle plumes” as widely used in current literature for convenience. The key is that the greater the heat/mass flux a plume has, the greater the effect of the plume-ridge interaction will be for a given plume-ridge distance and a given plate separation rate (see below).

### 9.2.2

#### Nature of Plume Materials

Compared to most Mid-Ocean Ridge basalts (MORBs), ocean-island basalts (OIB) are highly enriched in incompatible elements. Hofmann and White (1982) proposed that mantle plumes are from ancient oceanic crust. Many subsequent studies of OIB and enriched MORB favor this proposal, although some form of mantle metasomatism is clearly needed (Sun and McDonough 1989; Halliday et al. 1995; Niu et al. 1996 1999). Following the suggestion by Niu et al. (2002), Niu and O’Hara (see Sects. 7.4.2 and 7.5) using knowledge based on well-understood petrology, geochemistry and mineral physics demonstrate that ancient recycled oceanic crust cannot be the source material supplying OIB. Instead, they show deep portions of oceanic lithosphere that are the best candidates for mantle plume sources (Niu et al. 2002). These deep portions of oceanic lithosphere are filled with dykes or veins enriched in volatiles, alkalis, and all the other incompatible elements as a result of low-degree melt metasomatism at the interface between the low velocity zone and the cooling and thickening oceanic lithosphere. The

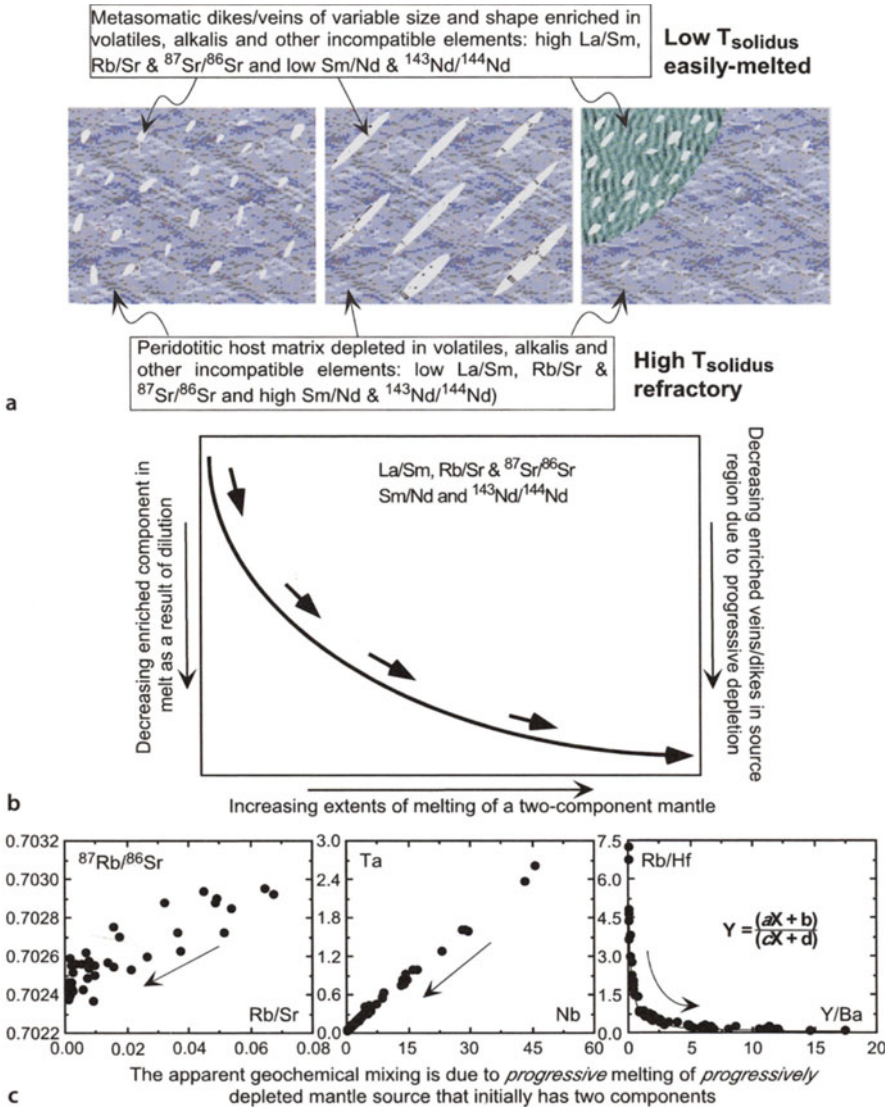


**Fig. 9.1.** **a** Schematic illustration of the concept of two-component fertile mantle sources, which include easily melted metasomatized dykes/veins of variable size and shape enriched in volatiles, alkalis and other incompatible elements dispersed in the refractory and predominantly depleted peridotite matrix. **b** Schematic illustration of the geochemical consequences of melting such a two-component mantle. The enriched dykes/veins have lower solidus temperatures and preferentially melt first. Consequently, the enriched component dominates the composition of the melt produced in the early stages and decreases with further melting as a result of dilution. Concurrently, the source region is progressively depleted in the enriched dykes/veins, and further melting of this depleted source material can only produce melts progressively depleted in volatiles and incompatible elements. **c** Three representative geochemical diagrams after Niu and Batiza (1997), showing apparent geochemical “mixing” as a consequence of the melting of a two-component mantle (or “melting-induced mixing”) (Niu et al. 1999, 2002). But, this is often mistakenly interpreted as “mixing” relationships between two singular melts or solids in the source regions of melt generation. The arrows in *Part c* point to the direction of increasing extents of melting

key is that plume sources (1) are peridotitic in bulk composition and (2) contain incompatible element-enriched dykes/veins of metasomatic origin. In other words, fertile OIB sources are composite lithologies with two components: an easily melted component enriched in volatiles, alkalis and other incompatible elements dispersed in the predominantly more refractory peridotitic matrix (Fig. 9.1a).

The concept of two-component fertile mantle sources favors the two-stage melting model for OIB and MORB (Phipps Morgan and Morgan 1999) and is consistent with observations in MORB from the eastern Pacific (Batiza and Vanko 1984; Batiza and Niu 1992; Zindler et al. 1984; Langmuir et al. 1986; Hekinian et al. 1989, 1995; Sinton et al. 1991; Niu et al. 1996, 1999, 2002; Niu and Batiza 1997; Niu and Hekinian 1997a; Regelous et al. 1999; Wendt et al. 1999) and the Mid-Atlantic Ridge (Niu and Batiza 1994; Niu et al. 2001; Regelous et al. 2001). In other words, both OIB and MORB sources have two such components, but the enriched dykes/veins are far more abundant in source regions of OIB than beneath ocean ridges (Niu et al. 1999). Figure 9.1b shows schematically that melting such a two-component mantle will produce more enriched melt during the early stage of melting not just because of the commonly perceived low-degree melting of a uniform source, but largely because of the greater contributions of the enriched easily melted component. With continued melting, the source region is progressively depleted in this enriched component, leading to a progressively more depleted melt. This is important in understanding the spatial variation of lava composition in the context of plume-ridge interactions (see below). The geochemical consequence of melting such a two-component mantle is to produce melting-induced mixing relationships (not true mixing between two singular end-members) in geochemical diagrams (Niu et al. 1996, 1999, 2002; Niu and Batiza 1997) (Fig. 9.1c).

This two-component fertile plume source model differs from the popular plume dispersion model (e.g., Schilling 1991). The latter model (1) assumes compositional and isotopic distinction between plume material and fertile MORB source material and (2) interprets the geochemical data as mixing between the two singular materials in the form of melt or in the source regions prior to the major melting events (Schilling 1991; Schilling et al. 1994, 1995, 1999; Kingsley et al. 2002). In our opinion, a dispersion model that requires an invasion of the plume material into the MORB source is physically difficult.

### 9.2.3

#### Ocean Ridges:

#### Ridge Suction – The Active Driving Force for Plume-Ridge Interactions

Ocean ridges are mostly passive features in the sense that mantle upwelling is largely caused by plate separation (McKenzie and Bickle 1998). This passive upwelling brings hot material from depths to melt by decompression (Fig. 9.2a,b). Continued plate separation leads to continued mantle upwelling, decompression melting, and crust formation. Furthermore, the oceanic lithospheric mantle, which thickens by cooling, is accreted fastest near ridges, with >50% of the full thickness achieved within the first ~17–18 Myr (Fig. 9.3a). All these factors require a continued asthenospheric material supply towards ocean ridges to form the lithosphere (crust plus lithospheric mantle). The entirety of the process is continuous, because the newly formed lithosphere is continuously moved away from the ridge. In other words, the asthenospheric mantle beneath ocean ridges represents the regions of lowest pressure in the entire mantle,

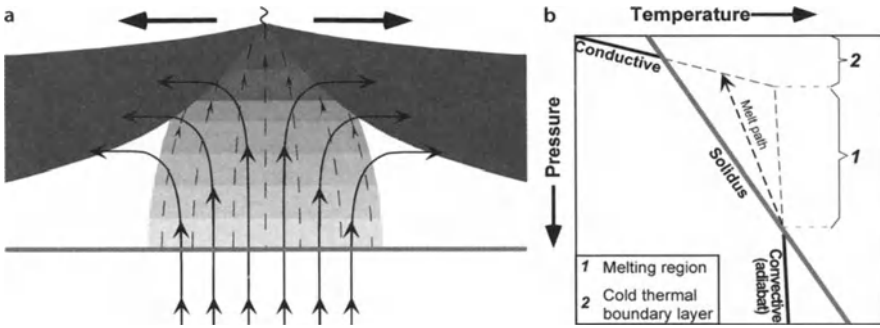
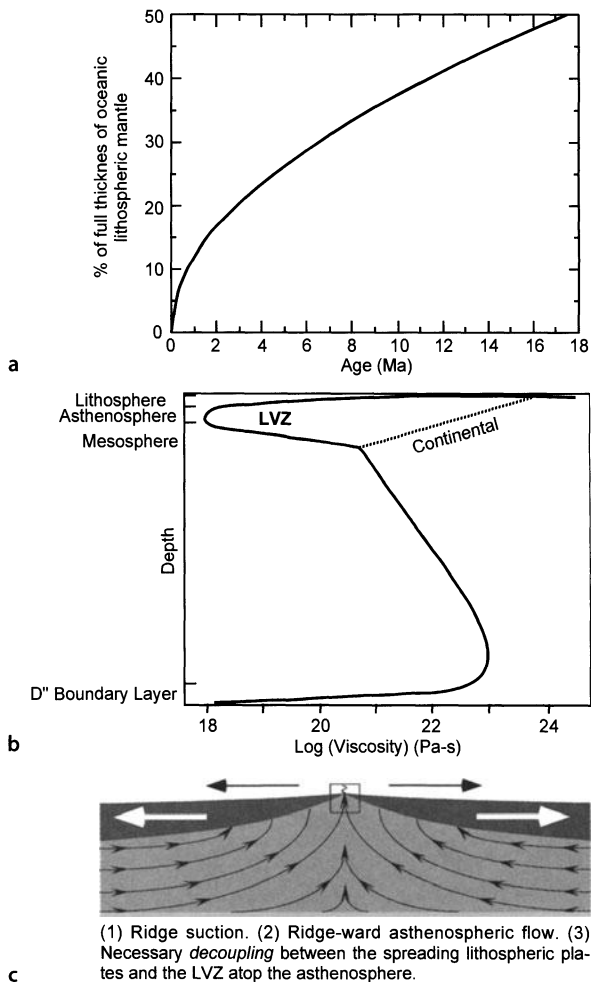


**Fig. 9.2.** **a** Cartoon showing plate separation-induced passive upwelling of the asthenospheric mantle and the resultant decompression melting beneath ocean ridges; **b** schematic illustration of the processes described in *Part a* in a P-T space. Passive upwelling brings hot mantle material to rise adiabatically and melt when encountering the solidus. Melting continues with upwelling until the upwelling mantle reaches the cold thermal boundary layer as a result of conductive heat loss to the surface (Niu 1997; Niu and Hekinian 1997b)

**Fig. 9.3.** **a** Assuming an oceanic plate reaches its full thickness (~95 km) after ~70 Myr (e.g., Stein and Stein 1997), ~50% of the lithospheric thickness is achieved in the first ~17.5 Myr (i.e.,  $t_{1/2} = (0.5 \times 70^{1/2})^2$ ). This, plus crust formation at ridges, requires ridgeward material supply. **b** As mantle viscosity is the lowest in the asthenosphere, in particular in the seismic low velocity zone (LVZ), at depths <~250 km, and increases exponentially with depth (Phipps Morgan et al. 1995; Lambeck and Johnston 1998), it is physically straightforward that the ridgeward mass flows must be mostly asthenospheric and horizontal. **c** Consequently, the regions of asthenosphere beneath ocean ridges have the lowest pressure that drives asthenospheric flows (i.e., ridge suction). This suggests that the spreading lithospheric plates are necessarily decoupled from the sublithospheric flow. The *square* at the ridge axis approximates the size of Fig. 9.2a



(1) Ridge suction. (2) Ridge-ward asthenospheric flow. (3) Necessary *decoupling* between the spreading lithospheric plates and the LVZ atop the asthenosphere.

which creates pressure gradients and sucks asthenospheric materials towards ocean ridges (Phipps Morgan et al. 1995; Niu et al. 1999). This argues that while ocean ridges are mostly passive features in the context of plate tectonics, they play an active role in dictating sublithospheric mantle flows.

The materials could either be supplied from below at great depths or transported laterally. As the mantle viscosity increases exponentially with depth beyond the low velocity zone (LVZ) (Fig. 9.3b after Phipps Morgan et al. 1995), it is physically straightforward that much of the material needed to create oceanic crust and oceanic lithosphere must be supplied by lateral sublithospheric flow through the LVZ (Niu et al. 1999). Mantle plume materials in the asthenosphere are generally hot (or “wet”), enriched in volatiles, and thus have the lowest viscosity. Consequently, mantle plume materials in the LVZ have the greatest tendency to flow and supply ridges because of the material needed beneath ocean ridges to form crust and lithospheric mantle (Niu et al. 1999). This is in fact apparent from mantle topographic studies (Zhang and Tanimoto 1993; Phipps Morgan et al. 1995). An inevitable conclusion of this analysis based on simple physics and mass conservation suggests that the lithospheric plate motion and the sublithospheric flow are necessarily decoupled (Fig. 9.3c), which is in fact seismically detected (Silver and Holt 2002).

## 9.2.4

### Ridge Suction Increase with Increasing Spreading Rate

The amount of material required per time unit to form oceanic lithosphere (crust plus lithospheric mantle) near ocean ridges increases linearly with an increasing spreading rate. This linear relationship is better understood if we consider the oceanic lithosphere that has reached its full thickness of ~95 km after 70 Ma (Stein and Stein 1996). As the full thickness is independent of spreading rate, the volume of the lithosphere ( $L$ ) formed per time unit per length unit parallel to the ridge would be the product of the half spreading rate ( $R_{1/2}$ ) and the full thickness ( $T_{\text{full}}$ ):  $L = R_{1/2} T_{\text{full}}$ . As  $T_{\text{full}}$  is constant,  $L$  is linearly proportional to  $R_{1/2}$  with  $T_{\text{full}}$  being the simple proportionality. A less straightforward, but equally valid and more relevant scenario is what is taking place in the vicinity of ocean ridges where oceanic lithosphere is being created. Figure 9.4a shows that within the first 1 Myr, the lithospheric mantle reaches a thickness of 11 km due to conductive cooling ( $L = 11 t^{0.5}$ ; see Fowler 1990). For a fast spreading ridge with  $R_{1/2} = 60 \text{ mm yr}^{-1}$ , the 1 Myr isochron is 60 km away from the ridge axis, but for a slow ridge with  $R_{1/2} = 10 \text{ mm yr}^{-1}$ , the 1 Myr isochron is 10 km from the ridge axis. The shaded areas are the lithospheric mantle thus far formed per unit length (per km along the ridge axis). For a half space, the volume of the lithospheric mantle formed per unit length in the first 1 Myr is  $440 \text{ km}^3$  beneath the fast ridge, but is only  $73.33 \text{ km}^3$  beneath the slow ridge. Again, a factor of 6 in volume,  $440 / 73.33 = 6$  is the same as the factor in spreading rate:  $60 / 10 = 6$ . If the width of the active upwelling zone beneath ocean ridges is proportional to the spreading rate (Turcotte and Phipps Morgan 1992; Forsyth 1992) and is about the width equivalent to 1 Myr isochron, then the total material flux towards the ridge can be calculated. Figure 9.4b shows the total material flux (in volume,  $\text{km}^3$ ) required to form the lithosphere on both sides of the ridge is linearly related to the spreading rate. Scenario A considers the material required to form the lithospheric mantle due only to conductive heat loss:  $\Phi (\text{km}^3) = 14.667 R_{1/2}$  ( $\text{km Myr}^{-1}$ ). Scenario B also includes a 5 km thick crust:  $\Phi (\text{km}^3) = 24.667 R_{1/2}$  ( $\text{km Myr}^{-1}$ ). Note that for simplicity it is assumed that the crust thickness is the same for both slow-

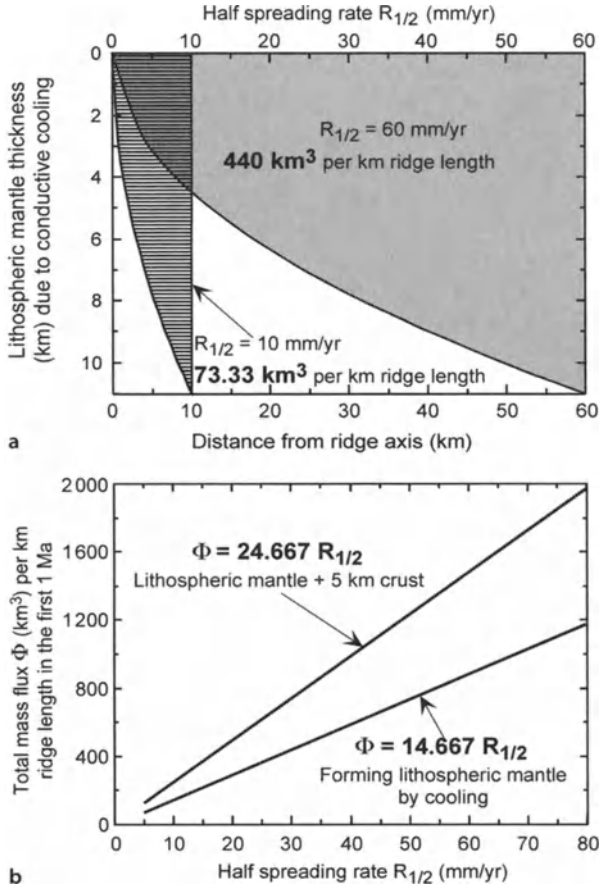


**Fig. 9.4.** a Comparison of materials (in km<sup>3</sup>) required to produce the lithospheric mantle on one side of the ridge in the first one million years between fast (e.g.,  $R_{1/2} = 60$  mm yr<sup>-1</sup>; shaded area times per unit ridge parallel length in km) and slow (e.g.,  $R_{1/2} = 10$  mm yr<sup>-1</sup>; area with zebra pattern times per unit length) spreading ridges. The volumes per unit length are calculated by simple integration of the shaded area:  $c \int_a^b \sqrt{x} dx$ , where  $x$  is the distance (km) from ridge axis  $a = 0$  to  $b$  of interest (60 km, and 10 km respectively here) and  $c = 11b^{-1/2}$  (km<sup>1/2</sup>). Note that the material requirement is linearly proportional to the spreading rate, i.e.,  $440 / 73.33$  (volume ratio) =  $60 / 10$  (speed ratio) = 6. b Indeed, the mass fluxes required to form the lithosphere are linearly related to spreading rate. Plotted are the total mass (km<sup>3</sup>) requirements across the ridge in the first one million years against half spreading rate. The total mass required to form the lithosphere as a result of conductive cooling is  $\Phi$  (km<sup>3</sup>) =  $15R_{1/2}$  (km Myr<sup>-1</sup>), and it becomes  $\Phi$  (km<sup>3</sup>) =  $25R_{1/2}$  (km Myr<sup>-1</sup>) if an average of 5 km thick crust is also considered. The important conclusion is that ridge suction force or ridgeward material flux is significant and increases with increasing spreading rate. Note that the calculations neglect the effect of density changes on the volume, but this effect is <2% and will not affect the conclusion here. Also note that the unit of the slope (~15 and 25 respectively) is km<sup>2</sup> Myr

and fast-spreading ridges here, which is incorrect in reality (Niu and Hekinian 1997b), but will not affect the conclusion here. This simple analysis indicates that the ridgeward mass flux, thus the ridge suction force, increases linearly with increasing plate-spreading rate.  $\Phi$  (km<sup>3</sup>) =  $25R_{1/2}$  (km Myr<sup>-1</sup>) is a good approximation (assuming a ~5 km thick igneous crust) for the material flux to the ridge in the first 1 Myr.

### 9.2.5 The Effect of Plume-Ridge Distance

Mantle plumes, by definition, are columnar ascending flows derived from the lower mantle (Morgan 1971, 1981). The lower-mantle derived plume materials melt by decompression in the asthenosphere (Campbell and Griffiths 1990) while spreading laterally away from plume centers beneath the lithosphere (Hill et al. 1992). The actual distance of lateral flow or spread is unknown, but is inferred to be less than 2 000 km from the geochemistry of volcanics and topographic expression in the context of plume-ridge interaction studies (Schilling 1991; Ito and Lin 1995; Ribe 1996; Sleep 1996). This inference is not unreasonable if plume materials are compositionally distinct from the shallow mantle materials as reflected in MORB and if plume materials are indeed significantly hotter than the ambient asthenospheric mantle. However, any further conclusions derived from such an inference can be dangerous without understanding (a) the very nature of plume materials; (b) the driving force for lateral sublithospheric flow; and (c) the possible differentiation of plume materials during the lateral flow. It is in fact very likely that plume materials may flow as far as physically possible, perhaps in excess of several thousands of km (see Niu et al. 1999). The important point here is the relative roles of ridges and plumes. If the plume-ridge distance is short, the interaction would be intense, to which plumes would contribute significantly in both mass and heat. On the other hand, if the plume is far from the ridge, the interaction would be weak, but the ridge would play a more important role in creating the pressure gradient needed to drive the ridgeward flow (Figs. 9.3a–3c and 9.4a–b).

## 9.3 Examples

### 9.3.1 “Proximal” Versus “Distal” Plume-Ridge Interactions

Iceland and Hawaii are presently the largest volcanically active mantle plumes/hotspots detected on modern ocean floor. The Iceland hotspot is centered on the very axis of the Mid-Atlantic Ridge (MAR), whereas the Hawaiian hotspot is a typical intraplate hotspot on the Pacific Plate some ~5 000 km away from the East Pacific Rise. If there are some kinds of plume-ridge interactions in both cases, then the style, intensity and both geological and geophysical consequences must be different.

MORB along the Reykjanes Ridge show incompatible element enrichment with an amplitude increasing systematically from N-type MORBs at deep ridges to enriched MORBs and even OIB compositions at shallow ridges toward Iceland (Sun et al. 1975; Schilling et al. 1983; Taylor et al. 1997). The along-ridge depth and the geochemical variations, which are the thermal and chemical consequences of plume ridge interactions (Schilling 1991; Ito and Lin 1995; Ito et al. 1996; Ribe 1996; Sleep 1996), reflect the along-ridge asthenospheric flow of plume materials (Fig. 9.5a). According to the popular plume dispersion model (Schilling 1991), the along-ridge variation in lava compositions would indicate the spatial extent of plume-ridge interactions. For example, geochemical signals of Iceland plume material in Reykjanes Ridge axial lavas decline and approach the level of N-MORB some ~1 500 km south of Iceland, which is thought

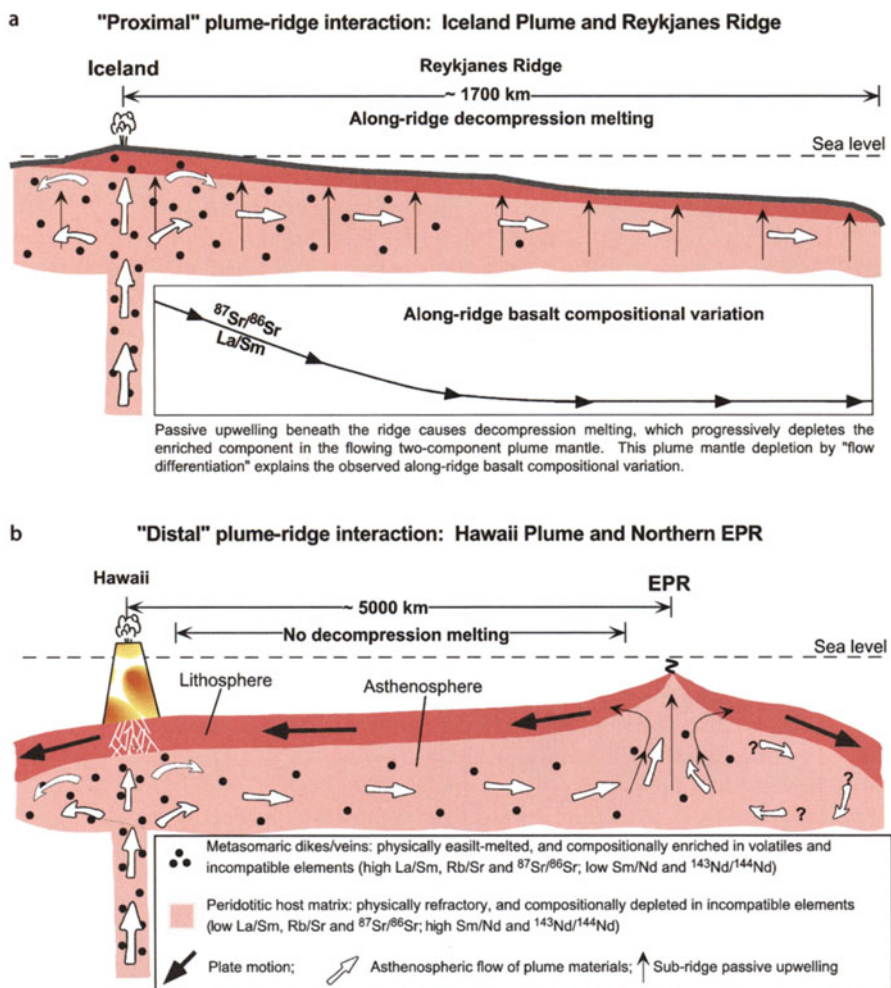


**Fig. 9.5.** Cartoons, modified from Niu et al. (1999), showing different consequences of plume-ridge interactions as a function of plume-ridge distance. If the plume is close to a ridge, for example, Iceland plume-Reykjanes Ridge, the buoyant upwelling and melting of the hot plume produces shallow ridge topography and enriched OIB-like basalt. The ambient sub-ridge mantle upwelling allows the plume material to flow laterally and to melt because of decompression, producing basalt whose extent of enrichment declines in the flow direction as the amount of the enriched component in the flowing plume mantle diminishes. The flow continues, but the enriched geochemical signals in the basalt do not. If the plume is far from a ridge, for example, Hawaiian plume-EPR, the low-viscosity Hawaiian plume material may flow laterally toward the EPR in response to the elevated ridge suction force beneath the fast-spreading EPR (Fig. 9.3a–3c and 9.4a,b). As the lateral flow is largely horizontal, decompression melting does not take place during flow, which allows the Hawaiian plume materials (both enriched and depleted) to survive long-distance transport to the EPR mantle

to be the maximum extent of the along-ridge effect of Iceland mantle plumes (e.g., Schilling 1991; Ito et al. 1996). This notion may be erroneous, since the depleted component of the plume material is likely to flow continuously. It is conceptually important to note that the declining geochemical enrichment in erupted lavas away from

Iceland is not the result of a simple dispersion or dilution effect, but the consequence of decompression melting during sub-ridge passive mantle upwelling, which preferentially melts and depletes the easily melted component within the remaining flowing plume material, leading to geochemically more depleted lavas erupted (Fig. 9.1b). The “residual” plume source materials depleted in enriched lithologies may continue to flow, but the “familiar” enriched geochemical signatures of plumes in erupted basalts diminish and are eventually replaced by “normal” depleted MORB.

Niu et al. (1999) termed this phenomenon as “flow differentiation” of an initially two-component plume mantle in a sub-ridge environment where the lithosphere is young and thin and decompression melting is possible because of the ambient passive mantle upwelling beneath the ridge (Fig. 9.5a). The increasing axial depth away from Iceland is the consequence of loss in both heat and mass (sub-ridge melting and cooling) of the plume material. The concept of a two-component plume source and “flow-differentiation” that we present here is physically straightforward and differs from the plume dispersion models (Schilling 1991; Ito et al. 1996; Schilling et al. 1999). The latter models, which require an “invasion” of enriched plume materials in the pre-existing depleted N-MORB mantle and a geochemical mixing between the two end-members, has space problems that are physically difficult to resolve.

Niu et al. (1999) showed that some enriched EPR MORBs define trends with the enriched end isotopically pointing to the field of Hawaiian lavas. This geochemical observation, plus mantle tomographic observation (Zhang and Tanimoto 1993; Phipps Morgan et al. 1995), led Niu et al. (1999) to suggest a sublithospheric flow of the Hawaiian mantle plume material towards the EPR (Fig. 9.5b). They termed such a physical scenario as “distal” plume-ridge interaction (versus the “proximal” interaction as in the case of Iceland-Reykjanes Ridge). This proposal would seem to be counter-intuitive because it requires some ~5 000 km sublithospheric flow in the LVZ against the vector of Pacific Plate motion. However, such lithosphere-asthenosphere decoupled flow in the LVZ is in fact physically straightforward (see above and Fig. 9.3a–c) because of ridge suction forces as a result of the material needs to form the crust and lithospheric mantle at ocean ridges. This is particularly the case beneath the fast-spreading EPR as the ridgeward mass flux increases with the increasing spreading rate (Fig. 9.4a,b). In contrast to the along-ridge flow of Iceland plume materials, which is focused along the ridge, the flow of Hawaiian mantle plume materials towards the EPR is more dispersed, which is unlikely to generate any significant thermal effect on the sea floor. However, as the asthenospheric flow is largely horizontal with essentially no decompression to cause melting, Hawaiian mantle plume materials (both enriched components and the depleted refractory peridotitic matrix) can survive a long distance travel to the EPR where they will melt by decompression and produce geochemically Hawaiian-like MORB (Niu et al. 1999).

### 9.3.2 Spreading Rate Directs Plume Flows

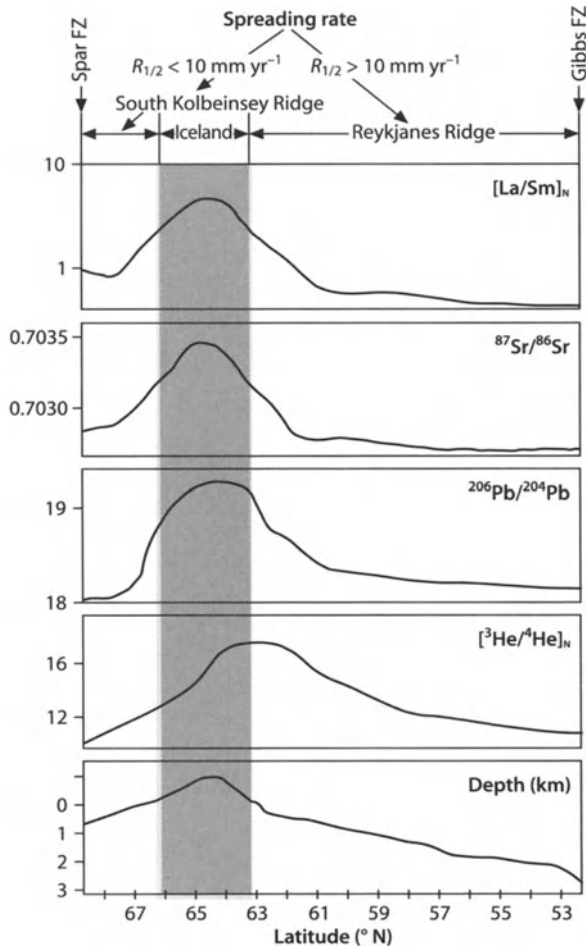
Figure 9.4 demonstrates that the ridge suction force or material needs/mass flux towards ridges increase with an increased spreading rate. As a result, plate-spreading rate plays a dictating role in both the direction and mass flux of plume material in the context of plume-ridge interactions. This explains many observations.

## 9.3.2.1

*Cases of Ridge-Centered Hotspots*

The along-ridge flow of Iceland plume material to both the north and south of Iceland (Mertz et al. 1991; Schilling et al. 1999) is asymmetrical. The apparent chemical and thermal effect of plume-ridge interaction extends more than  $\sim 1500$  km along the Reykjanes Ridge to the south (Schilling 1991; Ito et al. 1996), but it is no more than  $\sim 400$  km along the South Kolbeinsey ridge north of Iceland (Schilling et al. 1999). The total spreading rate along the Reykjanes Ridge increases from  $>20$  mm yr<sup>-1</sup> southward, whereas the total spreading rate north of Iceland decreases from  $<20$  mm yr<sup>-1</sup> northward. Therefore, the Icelandic plume materials prefer to flow along the Reykjanes ridge to the south of Iceland rather than to the north (Fig. 9.6) because of the greater material demand beneath the faster-spreading Reykjanes ridge than the slower-spreading Kolbeinsey ridge north of Iceland (Fig. 9.4). This asymmetrical effect of the Iceland plume, which we believe results from spreading rate differences, has been overlooked in all models of plume-ridge interactions.

**Fig. 9.6.** Schematic representation of topography (*bottom panel*) and geochemical trends of MORB along the North Mid-Atlantic Ridge to illustrate the asymmetrical effects of Iceland plumes. Geochemically, the Iceland plume has greater influence on the Reykjanes Ridge (RR) to the south both in amplitude and distance than on the South Kolbeinsey Ridge (SKR) to the north. The large topographic gradient from Iceland down to the Gibbs transform reflects the large thermal effect of the Iceland plume. The apparent shallower depth along the SKR is likely due to the thermal effect of the Jan Mayen plume to the north. We interpret the asymmetrical Iceland plume effect results from the greater spreading rate ( $>20$  mm yr<sup>-1</sup> full spreading rate) along the RR than the SKR, where the full spreading rate is  $<20$  mm yr<sup>-1</sup>. Greater spreading rate requires greater mass supply to form the lithosphere (Fig. 9.4). The schematic lava compositional variation is based on data given by Schilling et al. (1983, 1999) and Hanan et al. (2000)



Another example is the Amsterdam/St. Paul hotspots and their interactions with the Southeast Indian Ridge (Graham et al. 1999). Away from the hotspots, the plume-influenced topographic expression extends >3 000 km along the Southeast Indian Ridge down to the Australian-Antarctic Discordance, where the full spreading rate is on average >70 mm yr<sup>-1</sup>. However, the topographic expression is rather weak to the northwest, where the full spreading rate is <65 mm yr<sup>-1</sup>. A systematic sampling and large geochemical database with good spatial coverage is needed to evaluate the geochemical consequences.

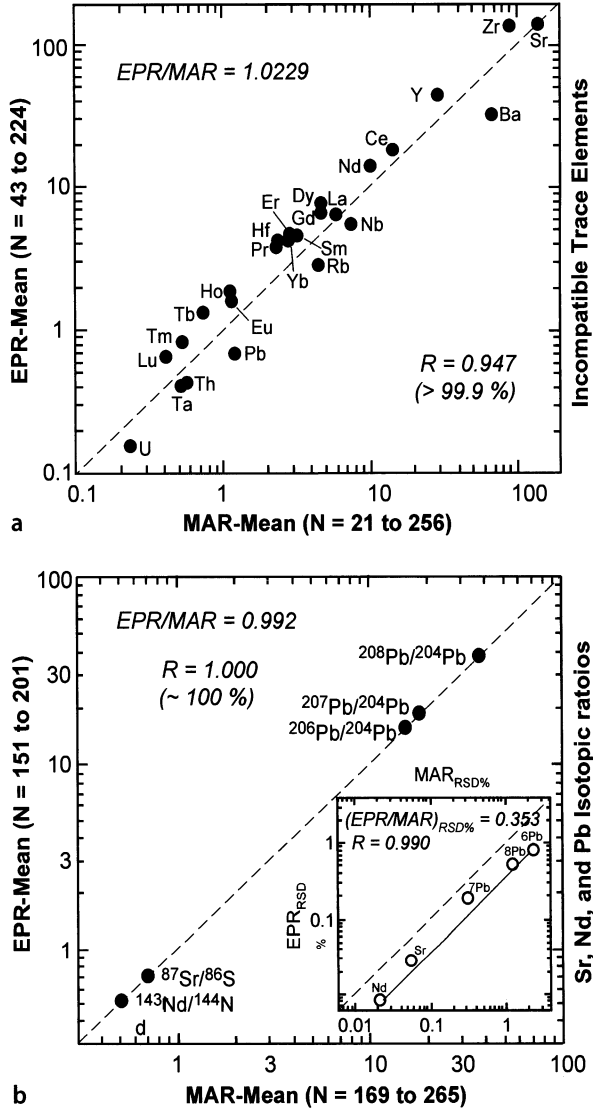
### 9.3.2.2

#### *The East Pacific Rise-Mid-Atlantic Ridge "Paradox"*

What is important in the context of plume-ridge interaction is the first-order differences between the fast-spreading EPR and the slow-spreading MAR. There are many topographically and geochemically identifiable mantle plumes/hotspots near the axis of the MAR (e.g., Iceland, Azores, 14° N anomalies, Ascension, Tristan, Gough, Shona, Bouvet and others), but the identifiable hotspots/plumes along the entire EPR are few, notably, the Easter hotspot at ~27° S on the Nazca plate. Such apparent unequal hotspot distribution would predict that enriched E-type MORB must be more abundant at the MAR than at the EPR. This is, however, not observed. In fact, along the MAR, away from those on- and near-axis hotspots/plumes and a few "wet" spots (e.g., Niu et al. 2001), the ridge segments are deep with depleted N-type MORB. In contrast, the EPR axis is generally shallow and enriched E-type MORBs occur along much of the axis where samples are available (Langmuir et al. 1986; Hekinian et al. 1989; Sinton et al. 1991; Batiza and Niu 1992; Reynolds et al. 1992; Perfit et al. 1994; Mahoney et al. 1994; Niu et al. 1996, 1999; Regelous et al. 1999). The EPR MORB and MAR MORB are compared in terms of average abundances of incompatible trace elements (Fig. 9.7a) and Sr, Nd and Pb isotopes (Fig. 9.7b) derived from the LDEO global MORB database (Lehnert et al. 2000). The statistically significant (>99.9% confidence level) linear correlation with close to unity slope (1.0229) (Fig. 9.7a) suggests that the mean abundance of incompatible trace elements in EPR and MAR MORB are quite similar. The highly incompatible elements such as Ba, Rb, Nb, Th, U, and Ta are plotted below the 1:1 line, suggesting that these elements are indeed slightly more abundant in MAR MORB than in EPR MORB while other elements are less so. However, as none of these elements deviate significantly from the 1:1 line, the overall abundance difference is insignificant. Note that the slope of 1.0229 suggests that on average EPR MORB have about 2% more incompatible elements as a whole than the MAR MORB, which is consistent with the greater extent of fractional crystallization in EPR MORB than in MAR MORB (Morel and Hekinian 1980; Natland 1980; Sinton and Detrick 1992). Figure 9.7b shows that isotopically the mean compositions of EPR and MAR MORB are identical. The relatively smaller variability (RSD% =  $1\sigma / \text{mean} \times 100$ ) of EPR MORB below the 1:1 is also consistent with the EPR MORB being more uniform in composition as a result of a greater extent of homogenization during melt aggregation in the mantle and magma chamber processes in the crust (Batiza 1984; Niu et al. 1996, 1999, 2002) at the fast-spreading ridges (Fig. 9.7b inset).

The similar mean MORB composition of EPR to that of MAR suggests similar extents of mantle plume contributions to EPR MORB. We consider the apparent rarity

**Fig. 9.7.** Comparison of mean abundances of incompatible elements in **a** and Sr-Nd-Pb iso-topic ratios in **b** between MORB from the fast-spreading EPR (23° S to 23° N) and the slow-spreading MAR (55° S to 52° N) using the recently available global MORB database (Lehnert et al. 2000). Note the statistically significant correlation with a nearly unity (1.0229) slope in Fig. 9.7a, suggesting similar plume material contributions to the two ocean-ridge systems. In Fig. 9.7b, the mean Sr-Nd-Pb isotopic ratios are statistically identical, which reinforces that plume source contributions are identical at the EPR and MAR. The correlated smaller variability (RSD% =  $1\sigma / \text{mean} \times 100$ ) of EPR MORB isotopic ratios plotted in the *inset* reflects a well-known effect of greater extents of melt homogenization in EPR MORB. The RSD% for incompatible element abundance is not correlated, thus not shown, which is largely due to inhomogeneity in data quality found in the literature (analyzed by different means in different laboratories with variable precisions and accuracy). Nd-Sr-Pb isotopes are all determined by TIMS normalized to international standards in all laboratories. Note that logarithmic scales are used to show all the details



of near-ridge hotspots along the EPR results from fast-spreading. The fast spreading creates large suction forces (Figs. 9.3c and 9.4) that do not allow the development of surface expressions of mantle plumes as such, but draw plume materials to a broad zone of sub-ridge upwelling, giving rise to abundant E-type MORB and elevated and smooth axial topography. This scenario applies to the Louisville hotspot-ridge interaction at the Pacific-Antarctic Ridge in the southern Pacific, where the exact location of the current Louisville hotspot center is difficult to identify (Lonsdale 1988) because of the significant ridge suction effect. However, both the thermal effects (shoaling axis:  $< 2000$  m below sea level) and geochemical consequences (abundant E-MORB and alkali basalts in near-ridges seamounts) of the plume-ridge interaction are conspicuous (Castillo et al. 1998).

The extensive EPR suction of plume materials is well expressed on the flanks of the southern EPR in the MELT region (Southern East Pacific Rise at 13° S–18° S; Forsyth et al. 1998), where both bathymetry and gravity display a conspicuous asymmetry across the axis with the Pacific Plate flank being much shallower, low in gravity, and importantly having many parallel volcanically active seamount chains perpendicular to the EPR axis. Some of these seamounts are volcanically active up to 150 km away from the EPR axis (Shen et al. 1995; Scheirer et al. 1996). We interpret these seamount chains as resulting from EPR suction of small mantle plumes (either hotspots or “wet” spots) beneath the Pacific Plate. These low viscosity plume materials must travel to the EPR because of the greater suction due to the high spreading rates in the area. The suction drives the flow to take the shortest path – perpendicular to the EPR axis. As the off-axis lithosphere is thin beneath the fastest spreading ridge and it is progressively thinner towards the axis, therefore the ridgeward flow of the plume materials has a component of decompression, which leads to decompression-melting and seamount formation. Predictably, (1) these seamounts must all be volcanically active, (2) most of these seamount lavas must be relatively enriched in volatiles, alkalis and other incompatible elements, and (3) the relative enrichment in lavas should decrease in seamounts closer to the axis because of progressive depletion of the easily melted components in the flowing plume material (Fig. 9.1b) as is the case along the Reykjanes Ridge (Fig. 9.5a). Petrological and geochemical data on samples with good spatial coverage are needed to test these predictions. In fact, the existing data along the Easter Seamount chain and the Foundation hotline elegantly illustrate this concept.

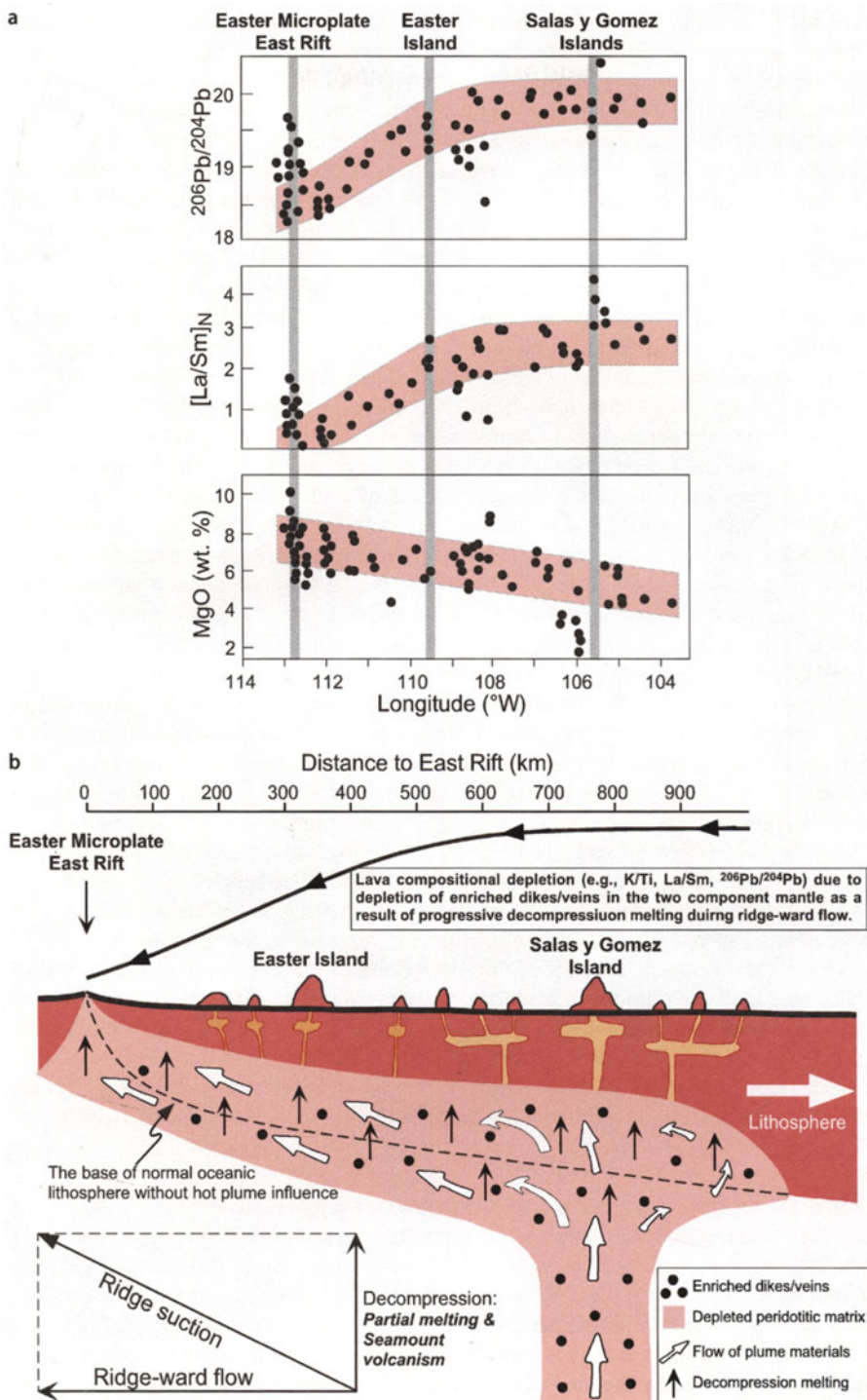
### 9.3.2.3

#### *Geochemical Expression of Plume-Ridge Interactions Along the Easter Seamount Chain*

The Easter Seamount chain (ESC) is located between Easter and Sala y Gómez islands and the East Rift of the Easter Microplate in the South East Pacific. This region has been well sampled and studied in recent years with the aim of understanding source compositions of the Easter mantle plume and the thermal and compositional linkage with the nearby EPR spreading center, which in this case is the East rift zone of the Easter microplate (Hanan and Schilling 1989; Fretzdorff et al. 1996; Haase and Devey 1996; Hekinian et al. 1996; Pan and Batiza 1998; Kingsley and Schilling 1998; Haase 2002; Kingsley et al. 2002). The ESC, also called Easter hotline, is composed of many volcanically active seamounts in a band with a width of ~150 km extending from the southern end of the East rift zone to the east for about ~900 km (Fig. 9.8a,b). Along the hotline are two conspicuous topographic anomalies marked by the Easter Island and the Sala y Gómez Islands, respectively about 400 km and 800 km away from the East Rift zone. The excess topography is proportional to the amount of melt delivered to the surface for volcanic constructions, and



**Fig. 9.8.** **a** Lava geochemical systematics along the Easter Seamount chain as a function of distance to the East Rift of the Easter Microplate. While scattered, most data define systematic trends as highlighted by the *shaded bands*. **b** Cartoon illustrating that the observed lava geochemical variation is the consequence of progressively melting a two-component plume material. Ridge suction requires the hot (or “wet”) plume material to flow towards the ridge with an upwelling component that causes decompression melting of the flowing plume material. The enriched dykes/veins with low solidus temperatures are progressively depleted during the ridgeward flow, thus leading to progressive melting of more depleted residual material and producing more depleted lavas towards the ridge (Fig. 9.1b,c). The geochemical data are from Pan and Batiza (1998), Kingsley et al. (1998, 2002), and the cartoon is modified from these authors



the amount of melt delivered to the surface is often considered to be the greatest over the hotspot center. Consequently, there has been a dispute about whether the present Easter hotspot is located beneath Easter Island (Haase and Devey 1996; Fretzdorff et al. 1996; Haase 2002) or is actually marked by the Sala y Gómez Islands (Hanan and Schilling 1989; Kingsley et al. 1998; Pan and Batiza 1998; Kingsley et al. 2002). Given the fact that ridge suction is the primary force that drives asthenospheric flow, it becomes physically straightforward to see that the ultimate hotspot source region must be located beneath the Sala y Gómez Islands or even to the east. If the hotspot source were beneath Easter Island, then an asthenospheric flow away from Easter Island to feed the volcanism of Sala y Gómez Islands is needed; however, there is no driving force for this flow direction. In fact, the systematic lava compositional variation (Pan and Batiza 1998; Kingsley et al. 1998, 2002) along the ESC as a function of distance to the East Rift zone supports the hypothesis that the actual hotspot is located beneath the Sala y Gómez Islands.

The scattered yet systematic declining in the enriched component towards the East Rift as indicated by geochemical parameters such as  $^{206}\text{Pb}/^{204}\text{Pb}$  and  $[\text{La}/\text{Sm}]_N$  (Fig. 9.8a; Also  $\text{K}/\text{Ti}$ ,  $\text{Na}_2\text{O}$ ,  $\text{K}_2\text{O}$ , and  $\text{CaO}/\text{Al}_2\text{O}_3$ , but not shown) is expectedly the consequence of “flow differentiation” discussed above (Figs. 9.1b and 9.5a). Note that a total spreading rate of this part of the EPR is about  $160 \text{ mm yr}^{-1}$ . As the Easter microplate rotates clockwise (Naar and Hey 1991), the East rift at the southeast corner (where the ESC meets) has a total spreading rate close to  $160 \text{ mm yr}^{-1}$ , thus having the greatest suction force for driving the asthenospheric flow of the Easter plume material. As the lithosphere is thinning towards the rift, this ridgeward asthenospheric flow also has a component of decompression (Fig. 9.8b). The latter inevitably leads to the partial melting of the flowing plume material beneath the lithosphere. The enriched dykes/veins of the plume source have lower solidus temperature, and will thus preferentially melt first, producing highly enriched lavas on the islands of Sala y Gómez. Decompression melting of the flowing plume material that is progressively depleted in the enriched and easily melted dykes/veins will produce melts that are progressively depleted in enriched components towards the East Rift as seen in erupted lavas (Fig. 9.8a). The physical mechanism is the same as described for lava geochemical signals along the Reykjanes Ridge – “flow differentiation” within the plume material that is flowing and melting. The ridgeward increase in MgO, which is proportional to eruption temperatures, results from composition-dependent melt evolution (Niu et al. 2002). Enriched melts are enriched in alkalis and volatiles that lower both the liquidus and solidus temperatures of silicate melts. Consequently, enriched melts cool to a lower liquidus temperature and crystallize to a greater extent (thus lower MgO) than depleted melts before solidification.

Our “flow-differentiation” model differs from the interpretations of a binary mixing between a distinctive (singular) plume source and the distinctive MORB source (Schilling 1991; Schilling et al. 1983, 1994, 1999; Kingsley et al. 1998, 2002). We emphasize that such ridgeward geochemical depletion in erupted lavas is an inevitable consequence of interaction between off-ridge mantle plumes and fast-spreading ridges. The same is also well expressed along the Foundation hotline volcanics (Hekinian et al. 1997, 1999) (see below). Note that the ridgeward flow of plume materials and the excess heat provided do not allow the normal development of the lithosphere by conductive cooling, thus leading to the thin lithosphere. This process is not the same as “thermal” erosion (Schilling 1991; Kincaid et al. 1995), which requires the pre-existence of a “perfect” lithosphere (as indicated by the *dashed line*) followed by erosion or channelization.

#### 9.3.2.4

#### *Geochemical Expression of Plume-Ridge Interactions Along the Foundation Hotline*

The Foundation Seamount chain is a fairly recent discovery (e.g., Mammerickx 1992; Devey et al. 1996; Hekinian et al. 1997, 1999) that extends northwestward for >1700 km from the inferred present-day location of the Foundation hotspot at  $\sim 36^\circ$  S,  $114^\circ$  W (Devey et al. 1996; Hekinian et al. 1997, 1999; O'Connor et al. 1998, 2001; Maia et al. 2000, 2001). The nature of the hotspot track is verified by the along-chain lava age progression (O'Connor et al. 1998, 2001) that is consistent with the notion that the Pacific Plate has spread northwestward at a speed of  $\sim 91 \pm 2$  mm yr<sup>-1</sup> for the last 21 Ma (O'Connor et al. 1998; see Sect. 11.5). The Foundation hotspot is inferred to be located in between  $\sim 35^\circ 45'$  S,  $114^\circ$  W and  $37^\circ 35'$  S,  $114^\circ 20'$  S with a radius of  $\sim 200$  km (Maia et al. 2001), and is about 400 km from the Pacific-Antarctic Ridge axis at  $\sim 37^\circ 45'$  S,  $111^\circ 7.5'$  W (Hekinian et al. 1999; Maia et al. 2001). The volcanically active seamounts between the PAR axis and the hotspot volcanoes form elongated volcanic ridges (Hekinian et al. 1997, 1999; O'Connor et al. 2001). These volcanically active ridges reveal a vivid expression of plume-ridge interaction between the Foundation hotspot and the Pacific-Antarctic Ridge. The systematic variation in the composition of these volcanics as a function of distance to the ridge axis shown in Fig. 9.9a is identical to that along the ESC (Fig. 9.8a) and is readily explained by the same process – ridge suction of the Foundation plume material that melts by decompression, and produces progressively more depleted lavas as a result of progressive depletion of easily melted dykes/veins in the rideward flowing plume material (Fig. 9.9b).

### 9.4

#### Summary and Conclusion

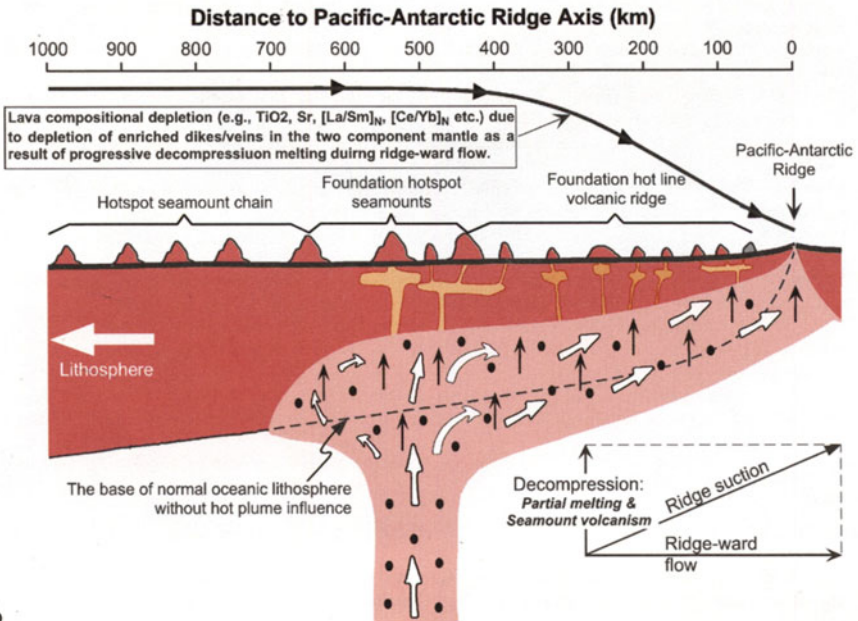
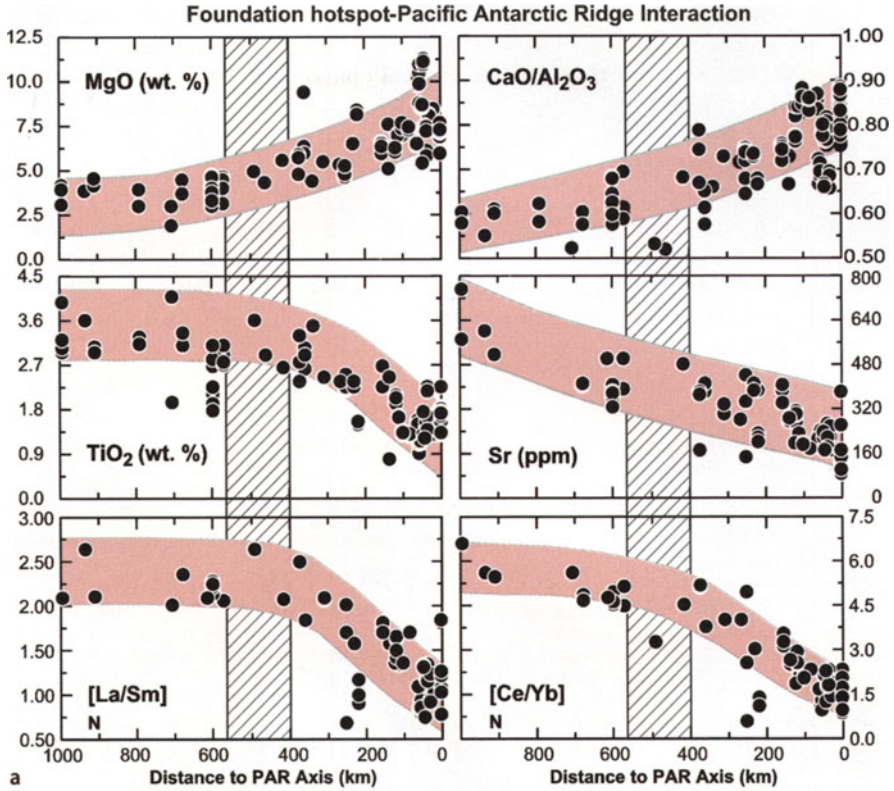
The main points of this contribution are listed below:

1. Plate tectonics and mantle plumes are genetically unrelated, but when the ascending mantle plumes approach lithospheric plates, interactions between the two occur. Such interactions are most prominent at or near ocean ridges, where the lithosphere is thin and the effect of mantle plumes is best revealed.
2. In order to fully understand plume-ridge interactions and their geophysical and geochemical expressions, some basic concepts must be understood and some variables must be considered. These include (a) the nature and composition of plume materials; (b) the actual role of ocean ridges; (c) the effect of plate spreading rate; and (d) plume-ridge distance.
3. Mantle plume materials are necessarily heterogeneous, and are likely to have two components: metasomatized, easily melted dykes/veins enriched in volatiles, alkalis and other incompatible elements dispersed in the more refractory, predominantly peridotitic matrix. Partial melting of such a two-component mantle produces geochemically enriched melts in its early stages, but progressive melting will produce progressively depleted melts because of progressive depletion of the enriched dykes/veins in the source regions. This is best manifested by systematic variations in lava composition (a) along the Reykjanes Ridge away from the Iceland, (b) along the Easter Seamount chain towards the East Rift, and (c) along the Foundation hotline volcanic ridges towards the Pacific-Antarctic Ridge.

4. While ocean ridges are mostly passive features in the context of plate tectonics, they play an active role in terms of plume-ridge interaction. This active role is manifested by the fact that the low velocity zone beneath ocean ridges represents regions of low pressure that allow asthenospheric flow (i.e., ridge suction). The ridge suction results from a need for material to form the oceanic crust and oceanic lithospheric mantle in the broad zone of upwelling beneath ocean ridges. The ridge suction or mass flux towards ocean ridges is linearly proportional to spreading rate.
5. Because the LVZ has the lowest viscosity that increases exponentially with depth, the mass flow towards ocean ridges is largely horizontal beneath the lithosphere. It follows that the spreading lithospheric plates must necessarily be decoupled from the sublithospheric flow. The degree of the decoupling increases with increasing plate spreading rate, because of the spreading-rate dependent material demand/flow towards the ridge.
6. The commonly interpreted geochemical “mixing” between compositionally distinct enriched plume material and depleted “MORB” source in the context of plume-ridge interaction is misleading. The apparent mixing relationship in geochemical diagrams is NOT a physical mixing either in the solid state or in the melt form, but the consequences of melting a two-component mantle. In other words, the so-called geochemical mixing is physically a differentiation of the two components from a composite lithology through partial melting.
7. The commonly perceived plume dispersion model, i.e., invasion of distinctively enriched plume materials into the depleted MORB mantle, has physical difficulties in making space available for the invasion. However, the “flow differentiation” model we present here in a sub-ridge or near-ridge environment is physically straightforward. Ridge suction requires that plume material flow towards the ridge. This ridge-ward flow has a decompression component that induces partial melting of the flowing plume material, which in turn will generate volcanic activities between hotspots and the nearby ridges (e.g., the Easter Seamount chain and Foundation hotline volcanic ridges). The ridge-ward flowing and melting plume material is progressively depleted in the enriched dykes/veins, resulting in the subsequent melts being progressively more depleted towards the ridge.
8. Because ridge suction increases with increasing spreading rate, ridge-centered mantle plumes, such as in Iceland, will have a greater thermal and compositional effect on the faster-spreading ( $>20 \text{ mm yr}^{-1}$ ) Reykjanes Ridge than the slower-spreading ( $<20 \text{ mm yr}^{-1}$ ) South Kolbeinsey Ridge to the north. The similar mean abundance of incompatible elements and identical mean Sr-Nd-Pb isotopic ratios between EPR MORB and MAR MORB suggest statistically similar plume material contributions to MORB melts in these two ocean-ridge systems. In contrast to the MAR, the rarity of near-ridge plumes along the EPR are due to its fast-spreading,



**Fig. 9.9. a** Geochemical systematics along the Foundation hotline volcanic ridges as a result of interactions between the Foundation plume and the Pacific-Antarctic Ridge near  $37^\circ \text{S}$ ,  $111^\circ \text{W}$ . The stippled columns mark the approximate location of Foundation hotspot seamounts. The data are from Hekinian et al. (1997, 1999) and Devey et al. (1997) with evolved samples (andesites, dacites and rhyolites having  $\text{SiO}_2 > 52 \text{ wt.}\%$ ) excluded. The data systematics and interpretations are the same as for the Easter hotline in Fig. 9.8a. Note that, in contrast to the systematics-defined by major and trace element data shown here, Pb isotopic data by Maia et al. (2001) show no systematics at all, which also contrasts with Pb isotopic systematics along the Easter hotline (Fig. 9.8a). **b** Cartoon showing essentially the same as in Fig. 9.8b



which results in extensive ridge suction forces or rideward mass flow and does not allow the development of surface expressions of small mantle plumes but incorporates them into the broad zone of mantle upwelling and fast oceanic crust accretion at the EPR.

## Acknowledgements

R. Hekinian acknowledges the Alexandre von Humboldt award and the Department of Geology, University of Kiel (Germany) for their support. Y. Niu thanks Cardiff University for support and UK NERC for support through a Senior Research Fellowship. Y. Niu also acknowledges the support from University of Houston for completing the research.

## References

- Batiza R (1982) Abundances, distribution and sizes of volcanoes in the Pacific Ocean and implications for the origin of non-hotspot volcanoes. *Earth Planet Sc Lett* 60:195–206
- Batiza R (1984) Inverse relationship between Sr isotope diversity and rate of oceanic volcanism has implications for mantle heterogeneity. *Nature* 309:440–441
- Batiza R, Niu Y (1992) Petrology and magma chamber processes at the East Pacific Rise ~9°30' N. *J Geophys Res* 97:6779–6797
- Batiza R, Vanko DA (1984) Petrology of young Pacific seamounts. *J Geophys Res* 89:11235–11260
- Campbell IH, Griffiths RW (1990) Implications of mantle plume structure for the evolution of flood basalts. *Earth Planet Sc Lett* 99:79–93
- Castillo PR, Natland JH, Niu Y, Lonsdale P (1998) Sr, Nd, and Pb isotopic variation along the Pacific ridges from 53 to 56° S: Implications for mantle and crustal dynamic processes. *Earth Planet Sc Lett* 154:109–125
- Davies GF, Richards MA (1992) Mantle convection. *J Geol* 100:151–206
- Deng J, Zhao H, Luo, Guo Z, Mo X (1998) Mantle plumes and lithosphere motion in east Asia. *Geodynam Ser* 27:59–66
- Devey CW, Hekinian R, Stoffers P, Ackermann D, Binard N, Drusch M, Francke B, Hémond C, Kapsimalis V, Lorenc S, Maia M, Möller H, O'Connor J, Perrot K, Pracht J, Ramm D, Rogers T, Statterger K, Steinke S, Victor P (1997) A first survey and sampling of the Foundation Seamount Chain. *Mar Geol* 137:191–200
- Duncan RA, Richards MA (1991) Hotspots, mantle plumes, flood basalts, and true polar wander. *Rev Geophys* 29:31–50
- Feighner MA, Richards MA (1995) The dynamics of plume-ridge and plume plate interactions: An experimental investigation. *Earth Planet Sc Lett* 129:171–182
- Forsyth DW (1998) Geophysical constraints on mantle flow and melt generation beneath mid-ocean ridges. AGU, Washington, D.C., *Geophys Monogr Ser* 71:1–66
- Forsyth DW, The MELT Seismic Team (1998) Imaging the deep seismic structure beneath a mid-ocean ridge: The MELT experiment. *Science* 280:1215–1218
- Fowler CMR (1990) *The solid Earth: An introduction to global geophysics*. Cambridge University Press Cambridge 472 pp
- Fretzdorff S, Haase KM, Garbe-Schonberg C-D (1996) Petrogenesis of lavas from the Umu volcanic field in the young hotspot region west of Easter Island, SE Pacific. *Lithos* 38:23–40
- Georgen JE, Lin J, Dick HJB (2001) Evidence from gravity anomalies for interactions of the Marion and Bouvet hotspots with the Southwest Indian Ridge: Effects of transform offsets. *Earth Planet Sc Lett* 187:283–300
- Graham DW, Johnson KTM, Priebe LD, Lupton JE (1999) Hotspot-ridge interaction along the Southeast Indian Ridge near Amsterdam and St. Paul Islands: Helium isotope evidence. *Earth Planet Sc Lett* 167:297–310
- Green DH, Falloon TJ (1998) Pyrolyte: A Ringwood concept and its current expression. In: Jackson I (ed) *The Earth's mantle – Composition, structure, and evolution*. Cambridge University Press, Melbourne, pp 311–380
- Hanan BB, Schilling J-G (1989) Easter microplate evolution: Pb isotope evidence. *J Geophys Res* 94: 7432–7448
- Hanan BR, Blichert-Toft J, Kingsley R, Schilling J-G (2000) Depleted Iceland mantle plume geochemical signature: Artifact of multicomponent mixing? *Geochem Geophys Geosy* 1 (article) 1999GC000009


- Haase KM (2002) Geochemical constraints on magma sources and mixing processes in Easter Microplate MORB (SE Pacific): a case study of plume-ridge interaction: *Chem Geol* 182:335–355
- Haase KM, Devey CW (1996) Geochemistry of lavas from the Ahu and Tupa volcanic fields, Easter Hotspot, Southeast Pacific: Implications for intraplate magma genesis near a spreading axis. *Earth Planet Sc Lett* 137:129–143
- Halliday AN, Dickin AP, Fallick AE, Fitton JG (1988) Mantle dynamics: A Nd, Sr, Pb and O isotope study of the Cameroon Line volcanic chain. *J Petrol* 29:181–211
- Halliday AN, Lee D-C, Tommasini S, Davies GR, Paslick CR, Fitton JG, James DE (1995) Incompatible trace elements in OIB and MORB source enrichment in the sub-oceanic mantle. *Earth Planet Sc Lett* 133:379–395
- Hanan BR, Blichert-Toft J, Kingsley R, Schilling J-G (2000) Depleted Iceland mantle plume geochemical signature: Artifact of multicomponent mixing? *Geochem Geophys Geosy* 1 (article) 1999GC000009
- Hekinian R, Thompson G, Bideau D (1989) Axial and off-axial heterogeneity of basaltic rocks from the East Pacific Rise at 12°35' N–12°51' N and 11°26' N–11°30' N. *J Geophys Res* 94:17437–17463
- Hekinian R, Bideau D, Herbért R, Niu Y (1995) Magmatic processes at upper mantle-crustal boundary zone: Garrett transform (EPR South). *J Geophys Res* 100:10163–10185
- Hekinian R, Francheteau J, Armijo R, Cogne JP, Constantin M, Girardeau J, Hey RN, Naar DF, Searl R (1996) Petrology of the Easter microplate region in the south Pacific. *J Volc Geotherm Res* 72:259–289
- Hekinian R., Stoffers P, Devey C, Ackermant D, Hémond C, O'Connor J, Binard N, Maia M (1997) Intraplate versus ridge volcanism on the Pacific Antarctic ridge near 37° S–111° W. *J Geophys Res* 94:12265–12286
- Hekinian R, Stoffers P, Ackermant D, Revillon S, Maia M, Bohn M (1999) Ridge-hotspot interaction: the Pacific-Antarctic Ridge and the foundation seamounts. *Mar Geol* 160:199–223
- Hill RI, Campbell IH, Davies GF, Griffiths RW (1992) Mantle plumes and continental tectonics. *Science* 256:186–193
- Hofmann AW, White WM (1982) Mantle plumes from ancient oceanic crust. *Earth Planet Sc Lett* 57:421–436
- Ito G, Lin J (1995a) Oceanic spreading center-hotspot interactions: Constraints from along-isochron bathymetric and gravity anomalies. *Geology* 23:657–660
- Ito G, Lin J (1995b) Mantle temperature anomalies along the present and paleoaxes of the Galapagos spreading center as inferred from gravity analyses. *J Geophys Res* 100:3733–3745
- Ito G, Lin J, Gable CW (1996) Dynamics of mantle flow and melting at a ridge-centered hotspot: Iceland and the Mid-Atlantic Ridge. *Earth Planet Sc Lett* 144:53–74
- Johnson RW (ed) (1989) Intraplate volcanism in eastern Australia and New Zealand. Cambridge University Press Melbourne, 408 pp
- Kincaid C, Ito G, Gable C (1995) Laboratory investigations of the interaction of off-axis mantle plumes and spreading centres. *Nature* 376, 758–761
- Kincaid C, Schilling J-G, Gable C (1996) The dynamics of off-axis plume-ridge interaction in the upper mantle. *Earth Planet Sc Lett* 137:29–43
- Kingsley R, Schilling J-G (1998) Plume-ridge interaction in the Easter-Salas y Gómez seamount chain-Easter microplate system: Pb isotope evidence. *J Geophys Res* 103:24159–24177
- Kingsley R, Schilling J-G, Dixon JE, Swart P, Poreda R, Simons K (2002) D/H ratios in basalt glasses from the Salas y Gómez mantle plume interacting with the East Pacific Rise: Water from old D-rich recycled crust or primordial water from the lower mantle? *Geochem Geophys Geosy* 1 (article) 2001GC000199
- Lambeck K, Johnston P (1998) The viscosity of the mantle: Evidence from analyses of glacial-rebound phenomena. In: Jackson I (ed) *The Earth's mantle – Composition, structure, and evolution*. Cambridge University Press, Melbourne, pp 461–502
- Langmuir CH, Bender JF, Batiza R (1986) Petrological and tectonic segmentation of the East Pacific Rise, 5°30'–14°30' N. *Nature* 332:422–429
- Lehnert K, Su Y, Langmuir CH, Sarbas B, Nohl U (2000) A global geochemical database structure for rocks. *Geochem Geophys Geosy* 1 (technical brief) 1999GC000026
- Lonsdale P (1988) Geography and history of the Louisville hotspot chain in the Southern Pacific. *J Geophys Res* 93:3078–3104
- Mahoney JJ, Sinton JM, Kurz DM, Macdougall JD, Spencer KJ, Lugmair GW (1994) Isotope and trace element characteristics of a super-fast spreading ridge: East Pacific Rise, 13–23° S. *Earth Planet Sc Lett* 121:173–193
- Maia M, Ackermant D, Dehghani GA, Gente P, Hekinian R, Naar D, O'Connor J, Perrot K, Phipps Morgan J, Ramillien G, Révillon S, Sabetian A, Sandwell D, Stoffers P (2000) The Pacific-Antarctic Ridge-Foundation hotspot interaction: A case study of a ridge approaching a hotspot. *Mar Geol* 167:61–84
- Maia M, Hémond C, Gente P (2001) Contrasted interactions between plume and lithosphere: The Foundation chain case. *Geochem Geophys Geosy* 1 (article), 2000GC000117

- McKenzie D, Bickle MJ (1988) The volume and composition of melt generated by extension of the lithosphere. *J Petrol* 29:625–679
- Mertz DF, Devey CW, Todt W, Stoffers P, Hofmann AW (1991) Sr-Nd-Pb isotope evidence against plume-asthenosphere mixing north of Iceland. *Earth Planet Sc Lett* 107:243–255
- Morel JM, Hekinian R (1980) Compositional variation of volcanics along segments of recent spreading ridges. *Contrib Mineral Petrol* 72:425–436
- Morgan JW (1971) Convection plumes in the lower mantle. *Nature* 230:42–43
- Morgan JW (1981) Hotspot tracks and opening of the Atlantic and Indian Oceans. In: Emiliani C (ed) *The sea*, vol. 7. Wiley, New York, pp 443–487
- Naar DF, Hey RN (1991) Tectonic evolution of the Easter microplate. *J Geophys Res* 96:7961–7993
- Natland JH (1980) Effect of axial magma chambers beneath spreading centers on the composition of basaltic rocks. *Init Rep Deep Sea Drill Proj* 54:833–850
- Niu Y (1997) Mantle melting and melt extraction processes beneath ocean ridges: Evidence from abyssal peridotites. *J Petrol* 38:1047–1074
- Niu Y, Batiza R (1994) Magmatic processes at the Mid-Atlantic ridge ~ 26° S. *J Geophys Res* 99:19719–19740
- Niu Y, Batiza R (1997) Trace element evidence from seamounts for recycled oceanic crust in the eastern equatorial Pacific mantle. *Earth Planet Sc Lett* 148:471–484
- Niu Y, Hekinian R (1997a) Basaltic liquids and harzburgitic residues in the Garrett transform: A case study at fast-spreading ridges. *Earth Planet Sc Lett* 146:243–258
- Niu Y, Hekinian R (1997b) Spreading rate dependence of the extent of mantle melting beneath ocean ridges. *Nature* 385:326–329
- Niu Y, Waggoner DG, Sinton JM, Mahoney JJ (1996) Mantle source heterogeneity and melting processes beneath seafloor spreading centers: The East Pacific Rise, 18°–19° S. *J Geophys Res* 101:27711–27733
- Niu Y, Collerson KD, Batiza R, Wendt I, Regelous M (1999) The origin of E-type MORB at ridges far from mantle plumes: The East Pacific Rise at 11°20' N. *J Geophys Res* 104:7067–7087
- Niu Y, Bideau D, Hekinian R, Batiza R (2001) Mantle compositional control on the extent of melting, crust production, gravity anomaly and ridge morphology: A case study at the Mid-Atlantic Ridge 33–35° N. *Earth Planet Sc Lett* 186:383–399
- Niu Y, Regelous M, Wendt JI, Batiza R, O'Hara MJ (2002) Geochemistry of near-EPR seamounts: Importance of *source vs. process* and the origin of enriched mantle component. *Earth Planet Sc Lett* 199:329–348
- O'Connor JM, Stoffers P, Wijbrans JR (1998) Migration rate of volcanism along the Foundation Chain, SE Pacific. *Earth Planet Sc Lett* 164:41–59
- O'Connor JM, Stoffers P, Wijbrans JR (2001) En echelon volcanic elongate ridges connecting intraplate Foundation Chain volcanism to the Pacific-Antarctic spreading center. *Earth Planet Sc Lett* 189:93–102
- Pan Y, Batiza R (1998) Major element chemistry of volcanic glasses from the Easter Seamount Chain: Constraints on melting conditions in the plume channel. *J Geophys Res* 103:5287–5304
- Perfit MR, Fornari DJ, Smith MC, Bender JF, Langmuir CH, Haymon RM (1994) Small-scale spatial and temporal variations in mid-ocean ridge crest magmatic processes. *Geology* 22:375–379
- Phipps Morgan J, Morgan JW (1998) Two-stage melting and the geochemical evolution of the mantle: A recipe for mantle plum-pudding. *Earth Planet Sc Lett* 170:215–239
- Phipps Morgan J, Morgan JW, Zhang Y-S, Smith WHF (1995) Observational hints for a plume-fed, suboceanic asthenosphere and its role in mantle convection. *J Geophys Res* 100:12753–12767
- Regelous M, Niu Y, Wendt JI, Batiza R, Greig A, Collerson KD (1999) An 800 ka record of the geochemistry of magmatism on the East Pacific Rise at 10°30' N: Insights into magma chamber processes beneath a fast-spreading ocean ridge. *Earth Planet Sc Lett* 168:45–63
- Regelous M, Niu Y, Castillo P, Batiza R, Greig A (2001) Contrasting geochemistry of on- and off-axis magmatism, 26° S Mid-Atlantic Ridge. *EOS Trans Am Geophys Union* 82(47):F1275–1276
- Reynolds JR, Langmuir CH, Bender JF, Kastens KA, Ryan WBF (1992) Spatial and temporal variability in the geochemistry of basalts from the East Pacific Rise. *Nature* 359:493–499
- Ribe NM (1996) The dynamics of plume-ridge interaction, 2: Off-ridge plumes. *J Geophys Res* 101:16195–16204
- Scheirer DS, Macdonald KC, Forsyth DW, Shen Y (1996) Abundant seamounts of the Rano Rahi Seamount Field near the Southern East Pacific Rise, 15° S to 19° S. *Mar Geophys Res* 18:13–52
- Schilling J-G (1991) Fluxes and excess temperatures of mantle plumes inferred from their interaction with migrating mid-ocean ridges. *Nature* 352:397–403
- Schilling J-G, Zajac M, Evans R, Johnston T, White W, Devine JD, Kingsley R (1983) Petrological and geochemical variations along the Mid-Atlantic Ridge from 29° N to 73° N. *Am J Sci* 283:510–586
- Schilling J-G, Hanan BB, McCully B, Kingsley RH, Fontignie D (1994) Influence of the Sierra Leone mantle plume on the equatorial Mid-Atlantic Ridge: A Nd-Sr-Pb isotopic study. *J Geophys Res* 99:12005–12028

- Schilling J-G, Ruppel C, Davis AN, McCully B, Tighe SA, Kingsley RH, Lin J (1995) Thermal structure of the mantle beneath Equatorial Mid-Atlantic Ridge: Inferences from spatial variations of dredged basalt glass composition. *J Geophys Res* 100:10057–10076
- Schilling J-G, Kingsley R, Fontignie D, Poreda R, Xue S (1999) Dispersion of the Jan Mayen and Iceland mantle plumes in the Arctic: A He-Pb-Nd-Sr isotope tracer study of basalts from the Kolbeinsey, Mohns, and Knipovich ridges. *J Geophys Res* 104:10543–10569
- Shen Y, Scheirer DS, Forsyth DW, Macdonald KC (1995) Trade-off in production between adjacent seamount chains near the East Pacific Rise. *Nature* 373:140–143
- Sinton JM, Detrick RS (1992) Mid-ocean ridge magma chambers. *J Geophys Res* 97:197–216
- Sinton JM, Smaglik SM, Mahoney JJ (1991) Magmatic processes at superfast spreading mid-ocean ridges: Glass compositional variations along the East Pacific Rise 13°–23° S. *J Geophys Res* 96:6133–6155
- Silver PG, Holt WE (2002) The mantle flow field beneath western north America. *Science* 295:1054–1057
- Sleep NH (1996) Lateral flow of hot plume material ponded at sublithospheric depths. *J Geophys Res* 101:28065–28083
- Stein S, Stein CA, (1996) Thermo-mechanical evolution of oceanic lithosphere: Implications for the subduction processes and deep earthquake. *AGU Geophys Monogr* 96:1–17
- Sun S-S, McDonough WF (1989) Chemical and isotopic systematics of ocean basalt: Implications for mantle composition and processes. *Geol Soc Spec Publ* 42:323–345
- Sun S-S, Tatsumoto M, Schilling J-G (1975) Mantle plume mixing along the Reykjanes ridge axis: Lead isotope evidence. *Science* 190:143–147
- Taylor RN, Thirwall MF, Morton JB, Hilton DR, Gee MAM (1997) Isotopic constraints on the influence of the Icelandic plume. *Earth Planet Sc Lett* 148:E1–E8
- Turcotte D L, Morgan JP (1992) Magma migration and mantle flow beneath a mid-ocean ridge. *AGU Geophys Monogr* 71:155–182
- Wendt JL, Regelous M, Niu Y, Hekinian R, Collerson KD (1999) Geochemistry of lavas from the Garrett transform fault: Insights into mantle heterogeneity beneath the eastern Pacific. *Earth Planet Sc Lett* 173:271–284
- Zhang M, Zhou X-H, Zhang J-B (1998) Nature of the lithospheric mantle beneath NE China: Evidence from potash volcanic rocks and mantle xenoliths. In: Flower MFJ, Chung S-L, Lo C-H, Lee T-Y (eds) *Mantle dynamics and plate interactions in East Asia*. AGU Washington, D.C., *Geodynam Ser* 27:197–219
- Zhang Y-S, Tanimoto T (1993) High-resolution global upper mantle structure and plate tectonics. *J Geophys Res* 98:9793–9823
- Zindler A, Staudigel H, Batiza R (1984) Isotope and trace element geochemistry of young Pacific seamounts: Implications for the scale of upper mantle heterogeneity. *Earth Planet Sc Lett* 70:175–195

Roger Hekinian  
Peter Stoffers  
Jean-Louis Cheminée  
Editors

# Oceanic Hotspots



Intraplate  
Submarine  
Magmatism  
and  
Tectonism



Springer

---

Roger Hekinian · Peter Stoffers · Jean-Louis Cheminée † (Eds.)

# Oceanic Hotspots

**Intraplate Submarine Magmatism  
and Tectonism**

With 217 Figures and 34 Tables



Springer

---

## Editors

*Dr. Roger Hekinian*

Keryunan, 29290 Saint Renan, France  
E-mail: hekinian@wanadoo.fr

*Dr. Jean-Louis Cheminée †*

*Prof. Peter Stoffers*

Institut für Geowissenschaften,  
Universität Kiel  
Olshausenstr. 40, 24098 Kiel, Germany  
E-mail: pst@gpi.uni-kiel.de

**Cover Montage** – Background: A three-dimensional map of the Pitcairn hotspot seafloor's volcanic landscape located in the South Pacific near 25°30' S–129°30' W using multibeam data processed by E. Le Drezen and A. Le Bot (IFREMER and GENAVIR). Overlay photographs (courtesy of IFREMER): An active hydrothermal chimney at 1457 m depth on top of the Teahitia Volcano (Society hotspot) and the submersible *Nautilus*.

ISBN 978-3-642-62290-8

### Library of Congress Cataloging-in-Publication Data data

Oceanic hotspots : intraplate submarine magmatism and tectonism / Roger Hekinian, Peter Stoffers, Jean-Louis Cheminée (eds.).

p. cm.

Includes bibliographical references and index.

ISBN 978-3-642-62290-8 ISBN 978-3-642-18782-7 (eBook)

DOI 10.1007/978-3-642-18782-7

1. Magmatism–Pacific Ocean. 2. Submarine geology. 3. Geology–Pacific Ocean. 4. Seamounts–Pacific Ocean. I. Hekinian, R. (Roger), 1935- II. Stoffers, P. (Peter) III. Cheminée, Jean-Louis.

QE461.028 2004  
551.46'814--dc22

Bibliographic information published by Die Deutsche Bibliothek  
Die Deutsche Bibliothek lists this publication in the Deutsche Nationalbibliografie;  
detailed bibliographic data is available in the Internet at <http://dnb.ddb.de>

This work is subject to copyright. All rights are reserved, whether the whole or part of the material is concerned, specifically the rights of translation, reprinting, reuse of illustrations, recitation, broadcasting, reproduction on microfilms or in any other way, and storage in data banks. Duplication of this publication or parts thereof is permitted only under the provisions of the German Copyright Law of September 9, 1965, in its current version, and permission for use must always be obtained from Springer-Verlag. Violations are liable for prosecution under the German Copyright Law.

[springeronline.com](http://springeronline.com)

© Springer-Verlag Berlin Heidelberg 2004

Originally published by Springer-Verlag Berlin Heidelberg New York in 2004

Softcover reprint of the hardcover 1st edition 2004

The use of general descriptive names, registered names, trademarks, etc. in this publication does not imply, even in the absence of a specific statement, that such names are exempt from the relevant protective laws and regulations and therefore free for general use.

Cover Design: Erich Kirchner

Dataconversion: Büro Stasch ([stasch@stasch.com](mailto:stasch@stasch.com)) · Bayreuth

Printed on acid-free paper – 32/3141 LT – 5 4 3 2 1 0